Sains Malaysiana 53(5)(2024): 983-994
http://doi.org/10.17576/jsm-2024-5305-01

Unlocking Therapeutic Potential: Identifying Small Molecule Inhibitors for SARS-COV-2 Variants' Main Protease (M^{PRO}) Through Molecular Docking Analysis

(Membuka Kunci Potensi Terapeutik: Mengenal Pasti Perencatan Molekul Kecil untuk Protease Utama (M^{PRO}) Varian SARS-COV-2 Melalui Analisis Dok Molekul)

CHONG YIE WOON[1,2] & NURUL IZZA ISMAIL[1,*]

[1]*School of Biological Sciences, Universiti Sains Malaysia, 11800 USM, Penang, Malaysia*
[2] *BiologicalDepartment of Chemistry, University of California Riverside, CA, USA*

Received: 3 November 2023/Accepted: 8 April 2024

ABSTRACT

Even with existing emergency drugs, the development of safer and more effective drugs for the treatment of COVID-19 still needs to continue. Virtual screening through a molecular docking approach is a powerful way to discover potential compounds for new drug discovery. In this study, we targeted SARS-CoV-2 wild-type major protease (M^{Pro}), beta, lambda and omicron variants, to conduct a virtual screening with a selection of 100 ligands from the PubChem database using AutoDock Vina software. Among the inhibitors that have been identified are ten compounds consisting of ergotamine, 2,5-Dibenzyloxy-3-hydroxyligand-hexanedioic acid bis-[(2-hydroxy-indan-1-YL)-amide], remetinostat, benzamidine, argifin, irinotecan, dihydroergotamine, telmisartan, bromocriptine, and cilengitide, which exhibited the highest binding affinity. Interaction analysis through BIOVIA Discovery Studio showed the binding and interaction modes between these inhibitors and M^{Pro} residues of the variant. This mainly refers to 2,5-Dibenzyloxy-3-hydroxyligand-hexanedioic acid bis-[(2-hydroxy-indan-1-YL)-amide] and remetinostat which consistently exhibit strong interactions with M^{Pro} variants. This research provides promising leads for the development of potential COVID-19 therapeutics. In summary, targeting conserved M^{Pro} with small molecule inhibitors provides a solid foundation for combating SARS-CoV-2 and its variants, holding promise for effective COVID-19 mitigation.

Keywords: COVID-19; molecular docking; M^{Pro}; remetinostat; 2,5-Dibenzyloxy-3-hydroxyligand-hexanedioic acid bis-[(2-hydroxy-indan-1-YL)-amide]

ABSTRAK

Walaupun dengan ubat kecemasan yang sedia ada, pembangunan ubat yang lebih selamat dan berkesan untuk rawatan COVID-19 masih perlu diteruskan. Penyaringan maya melalui pendekatan dok molekul merupakan satu cara yang terbaik untuk penemuan sebatian yang berpotensi bagi penemuan ubat baharu. Dalam kajian ini, kami menyasarkan protease utama (M^{Pro}) jenis liar SARS-CoV-2, beta, lambda dan varian omikron, untuk dijalankan saringan maya dengan pemilihan 100 ligan daripada pangkalan data PubChem menggunakan perisian AutoDock Vina. Antara perencat yang telah dikenal pasti adalah sepuluh sebatian terdiri daripada ergotamin, 2,5-Dibenzyloxy-3-hydroxyligand-hexanedioic acid bis-[(2-hydroxy-indan-1-YL)-amide], remetinostat, benzamidine, argifin, irinotecan, dihydroergotamine, telmisartan, bromocriptine dan cilengitide yang menunjukkan pertalian pengikatan tertinggi. Analisis interaksi melalui BIOVIA Discovery Studio mendedahkan mod pengikatan dan interaksi antara perencat ini serta sisa M^{Pro} bagi varian tersebut. Ini terutamanya merujuk kepada 2,5-Dibenzyloxy-3-hydroxyligand-hexanedioic acid bis-[(2-hydroxy-indan-1-YL)-amide] dan remetinostat yang secara tekalnya menunjukkan interaksi yang kuat dengan varian M^{Pro}. Penyelidikan ini memberikan petunjuk yang berpotensi untuk pembangunan terapeutik COVID-19. Ringkasnya, menyasarkan M^{Pro} yang dipelihara dengan perencat molekul kecil menyediakan asas yang kukuh untuk memerangi SARS-CoV-2 dan variannya, memegang janji untuk mitigasi COVID-19 yang berkesan.

Kata kunci: COVID-19; dok molekul; M^{Pro}; remetinostat; 2,5-Dibenzyloxy-3-hydroxyligand-hexanedioic acid bis-[(2-hydroxy-indan-1-YL)-amide]

INTRODUCTION

Severe Acute Respiratory Syndrome Coronavirus-2 (SARS-CoV-2) is the virus responsible for the COVID-19 pandemic, caused by the novel coronavirus. Since its emergence in late 2019, the virus has spread globally, leading to significant morbidity and mortality. Developing effective strategies to combat SARS-CoV-2 is critical in controlling the pandemic and reducing its impact on public health and economies worldwide.

One promising approach in combating SARS-CoV-2 is targeting the virus's main protease (M^{Pro}), also known as 3-chymotrypsin-like protease ($3CL^{Pro}$) (Lee et al. 2020). M^{Pro} plays a crucial role in the viral life cycle by processing viral polyproteins, which are essential for viral replication (Li et al. 2020). Inhibition of M^{Pro} can potentially disrupt viral replication and reduce the spread of the virus within the host (Adedeji & Sarafianos, 2014; Anand et al. 2003; Li et al. 2020; ul Qamar et al. 2020). The monomeric form of M^{Pro} is illustrated in Figure 1.

A key advantage of targeting M^{Pro} is its relatively conserved nature among different SARS-CoV-2 variants (Goyal & Goyal 2020; Morse et al. 2020). While the virus has undergone mutations, particularly in the spike protein, the main protease remains relatively stable. While the main protease (M^{Pro}) of most SARS-CoV-2 variants has mutations in their catalytic sites, like G15S in C.37 Lambda, T21I in B.1.1.318, L89F in B.1.2, K90R in B.1.351 Beta, L205V in P.2 Zeta, and P132H in B.1.1.529 Omicron, these mutations only slightly (10-15%) affect their function. Importantly, the active sites of these enzymes remain effective targets for small molecule inhibitors to block their activity. This conservation makes M^{Pro} an attractive target for drug development, as inhibitors targeting this enzyme could potentially be effective against multiple variants of the virus (Li et al. 2020; Xiong et al. 2020).

Most serine proteases contain a catalytic triad of SER-HIS-ASP, however, SARS-CoV-2 M^{Pro} is unique in the case that the virus possesses a CYS-HIS catalytic dyad. Surrounding the catalytic residues, some important binding residues help make up the M^{Pro} active site and contribute to the functional relevance. They are residues HIS 41, SER 46, CYS 145, LEU 141, ASN 142, GLU 166, PRO 168, GLN 189, THR 190, and ALA 191 (Figure 2) (Kneller et al. 2020) which formed the catalytic pocket of SARS-CoV-2 M^{Pro}. Apart from that, they serve as enzyme catalytic site. Understanding the atomic constituents of the binding site and the enzyme catalytic mechanism are necessary to identify the active site of the structure.

Since the SARS outbreak in 2002, academics and biopharmaceutical companies have been submitting patents for M^{Pro} small molecule inhibitor approaches (Chia, Xu & Shuyi Ng 2022). Since the emergence of the pandemic, several repurposed drugs used to target other diseases have been employed as inhibitors for M^{Pro}. Paxlovid by Pfizer is a repurposed drug with inhibition properties against the SARS-CoV-2 M^{Pro}, licensed for emergency use by the FDA with strict dosage control. Initially developed in 2005 to combat the SARS outbreak, Paxlovid's effectiveness stems from its inhibition of mature viral proteins via nirmatrelvir (PF-07321332) and stability enhancement through ritonavir (Hung et al. 2022). But Paxlovid is not recommended for patients with liver or renal dysfunction, those requiring daily medications, or immune-compromised individuals. Despite these limitations, clinical trials demonstrate Paxlovid's high efficacy (89%) in preventing severe complications in vulnerable COVID-19 patients (Pang et al. 2023).

Some studies show nirmatrelvir inhibits the peptidomimetic of M^{Pro}, while rupintrivir blocks between two catalytic residues in the protease (Lam & Patel 2023; Vatansever et al. 2021). Sometimes, nirmatrelvir is co-administered with ritonavir to enhance the drug's effect. Additionally, HIV protease inhibitors like lopinavir/ritonavir have been of particular interest in inhibiting SARS-CoV-2 by binding to M^{Pro} (Nutho et al. 2020). All these drugs blocking the protease's catalytic mechanism. However, these drugs have drawbacks, including toxicity side effects or poor efficacy (Khalifa & Al Ramahi, 2024). Additionally, nirmatrelvirin, the primary inhibitor for M^{Pro} used extensively to treat SARS-CoV-2 patients, was found to bind less effectively to the mutated protein in a recent study (Flynn et al. 2023).

During the early stages of the outbreak, the antiviral hydroxychloroquine was listed as an emergency therapeutic agent. However, test outcomes on its efficacy were inconsistent, leading the Food and Drug Administration (FDA) to remove hydroxychloroquine from the list. Subsequently, other drugs such as remdesivir, lopinavir/ritonavir, and dexamethasone were approved for emergency use to treat COVID-19 symptoms. However, later studies indicated less therapeutic effect and more side effects in patients, with outcomes being less consistent (Khalifa & Al Ramahi 2024). This situation has driven the need for drug repurposing, aiming to quickly identify small molecules with high therapeutic efficacy and effectiveness, while minimizing toxicity effects.

To the best of our knowledge, no highly effective drug specifically targeting the SARS-CoV-2 M^{Pro} has been approved yet. However, the FDA has authorized certain drugs for emergency use in critically ill patients needing ventilators. These drugs were not developed for COVID-19 but are repurposed. This highlights the ongoing challenges for scientists in discovering a suitable inhibitor for this critical viral enzyme. This is precisely why we are proceeding with this study, aiming to contribute to the

development of potential therapeutics against SARS-CoV-2. This research aims to find inhibitors for SARS-CoV-2 variants. Traditional lab methods are slow and costly for designing new drugs. Virtual screening helps find potential drugs faster and more efficiently. Testing these inhibitors in labs can show more about their effectiveness. This research not only fights COVID-19 but also prepares us for future viral threats.

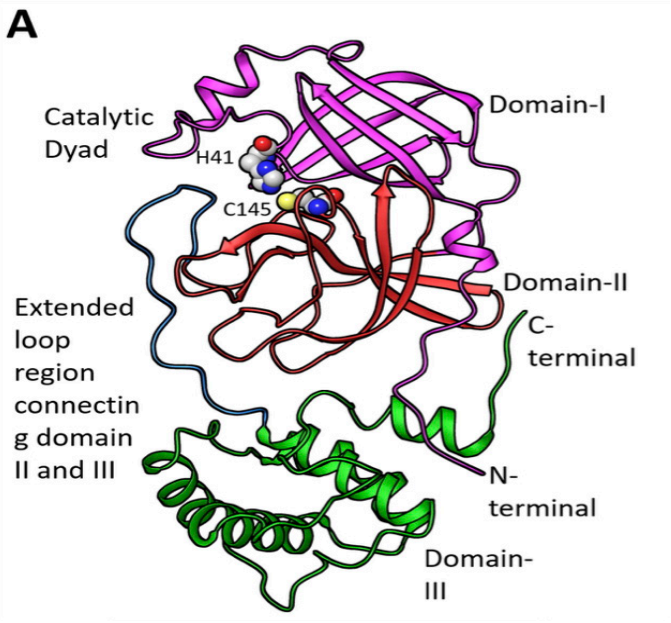

FIGURE 1. Two-dimensional view of the SARS-CoV-2 main protease, M^{Pro} monomeric (inactive) structure. Domains I, II, and III make up the structure, with the catalytic dyad positioned between Domains I and II comprising conserved catalytic residues Histidine 41 and Cysteine 145. Adapted from Mittal et al. (2021), Figure 1(A)

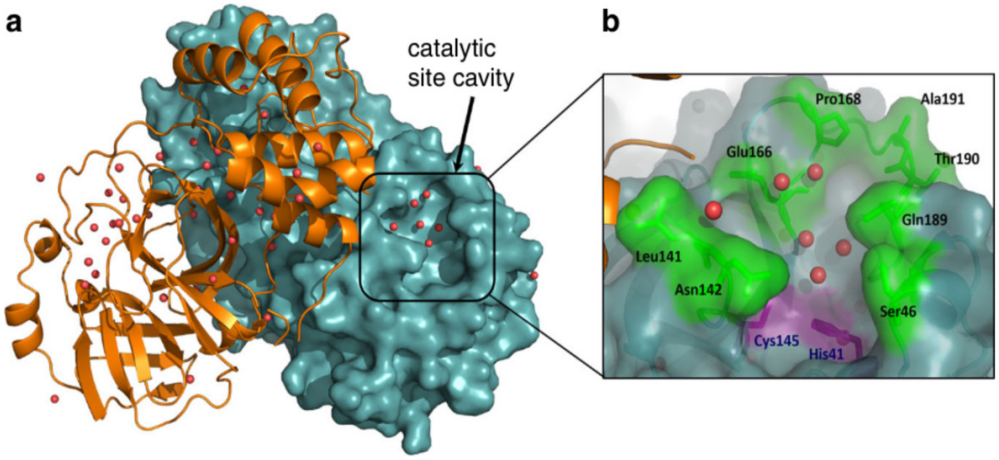

FIGURE 2. A zoom-in version of the catalytic site cavity of a SARS-CoV-2 M^{Pro} monomer. HIS 41 and CYS 145 are the catalytic residues, surrounded by binding residues, SER 46, LEU 141, ASN 142, GLU 166, PRO 168, GLN 189, THR 190 and, ALA 191. The water molecules are represented by red spheres. Adapted from Kneller et al. (2020), Figure 1

MATERIALS AND METHODS

The 3D structures of SARS-CoV-2 protein, wild type and mutant type were retrieved from the Protein Data Bank (RCSB PDB). Virtual screening of the compatible and potential small ligands/drugs were performed on small molecule database retrieved from PubChem. Molecular docking of the potential inhibitors on the SARS-CoV-2 targeted active site was run via AutoDock Vina v1.2.2. Configuration and interaction of the virus active site and the inhibitors were visualised and analysed via PyMOL and BIOVIA discovery studio visualizer. A methodology flowchart is shown in Figure 3.

3D STRUCTURE OF SARS-COV-2 MAIN PROTEASE (M^{PRO})

The 3D structures of SARS-CoV-2 M^{Pro} of wild and mutant types were retrieved from the Protein Data Bank (PDB) database. The PDB is a free online database that grants access to biological marcomolecules' 3D structures. Each protein in the PDB is assigned a unique accession code for identification: wild M^{Pro} (PDB ID: 6Y2E at 1.75 Å resolution) (Bzówka et al. 2020; Zhang et al. 2020), beta M^{Pro} (PDB ID: 7U29 at 2.09 Å resolution), lambda M^{Pro} (PDB ID: 7U28 at 1.68 Å resolution), and omicron M^{Pro} (PDB ID: 7TLL at 1.63 Å resolution) (Greasley et al. 2022). The 3D structures of the targeted protein can be obtained by simply applying the PDB ID or by using keywords such as the SARS-CoV-2 main protease variant name, allowing you to refine your search and find specific information related to mutations or variants of the main protease of SARS-CoV-2. Using the PBD ID obtained from the literature, wild and mutant M^{Pro} files were downloaded in the PDB format, a standard for macromolecular structure data obtained from X-ray diffraction and NMR experiments (Muppalaneni & Rao 2011).

VIRTUAL SCREENING OF POTENTIAL LIGANDS

Small molecule ligands were screened from PubChem (https://pubchem.ncbi.nlm.nih.gov). Total number of 100 potential inhibitors were chosen for mass screening. These compounds were filtered based on a few criteria: small molecular weight below 900 Da (Govardhanagiri Bethi & Nagaraju 2019; Higueruelo et al. 2009; Xiang et al. 2022), structure similarities based on the WHO-approved emergency medications for COVID-19 (Huang et al. 2018), antiviral, and protease inhibition properties. The 3D conformers of the 100 compounds available in Structure Data File (SDF) files were downloaded individually from PubChem. The information concerning atoms, bonds, connections, and molecular coordinates were retrieved in SDF format for ligands (Muppalaneni & Rao 2011).

MOLECULAR DOCKING PROTOCOL

Receptor preparation and Grid mapping

The 3D structure of the SARS-CoV-2 wild type M^{Pro} (PDB ID: 6Y2E) was loaded onto AutoDockTools (ADT) from

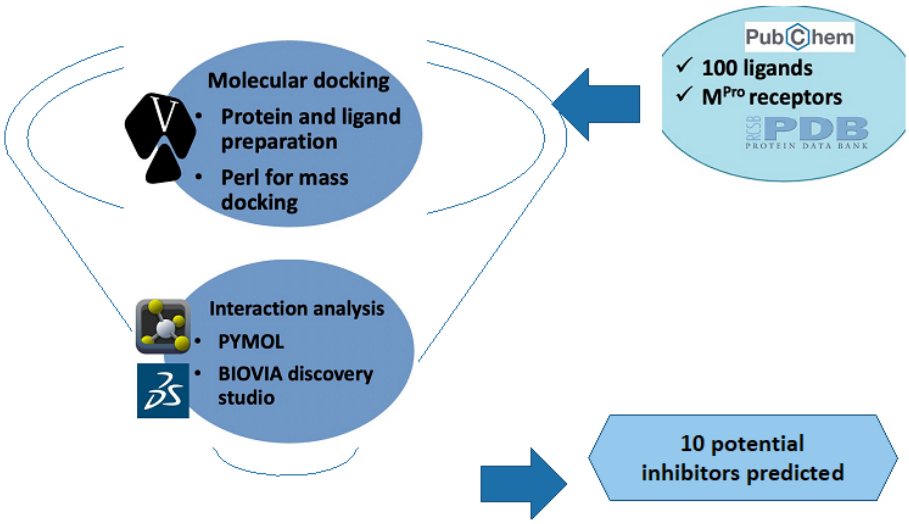

FIGURE 3. Flowchart summarises the process of this study

the retrieved PDB file. Water molecule was deleted to show the receptor's binding pocket and minimise unfavourable interactions that could impact the score result (Gentile et al. 2022). The M^{Pro} receptor chain B was deleted, while chain A was retained for docking since it contains active amino acid residues (Khan et al. 2021; Odhar et al. 2020). Often, the presence of missing residues in downloaded PDB file is encountered (Ordog, Szabadka & Grolmusz 2009). ADT is equipped with the missing residue repair action to repair the missing atoms. Next, to determine atom types for scoring purposes, AutoDock Vina v1.2.2 requires polar (possibly hydrogen bonding) hydrogens. The phase was established by adding polar hydrogen only. Kollman Charges was added to emulate the protein in the natural state.

The amino acid residues that flank the catalytic cavity were highlighted on the "R" column. They are HIS 41, SER 46, CYS 145, LEU 141, ASN 142, GLU 166, PRO 168, GLN 189, THR 190, and ALA 191 (Kneller et al. 2020). To make the receptor's binding pocket visible, 6Y2E's other atoms were kept concealed. The Grid Box measurement was manually adjusted to cover all of the residues shown. Grid box data were recorded for the subsequent operation. Lastly, the receptor has been prepared and was ready to be saved as "6Y2E.pdbqt" file, as required by AutoDock Vina v1.2.2. The same procedure of receptor preparation was applied to beta M^{Pro} (PDB ID: 7U29), lambda M^{Pro} (PDB ID: 7U28), and omicron M^{Pro} (PDB ID: 7TLL). In prior to that, the attached ligand on these 3D structures would have to be removed.

Ligands preparation via Open Babel GUI

Using Open Babel GUI 2.3.1 (https://openbabel.org/docs/dev/Installation/install.html), the ligands in "sdf" format were converted to "pdbqt" format. The "INPUT FORMAT" and "OUTPUT FORMAT" were ensured to be "sdf -- MDL MOL format" and "pdbqt – AutoDock PDBQT format", respectively. The "ligand1.sdf" file was loaded under "INPUT FORMAT" on the left tool bar, while "ligand1.pdbqt" was named under the "OUTPUT FORMAT" on the right tool bar. Then, by clicking the "CONVERT" on the top centre column, the conversion was said to be completed for the first ligand. The same procedure was used to convert the files for the remaining 99 ligands.

Grid box

The grid box figures retrieved from the final step of the receptor preparation included the x, y, z of center and size. A "conf_vs.txt" text document file was created using Notepad to provide docking instruction to AutoDock Vina v1.2.2. For wild M^{Pro} receptor, the center (-14.799, -25.606, 0.936) of the search space has been determined on the bases of the bound small molecule ligand, and its size has been set to 98×88×114 Angstroms to cover the active site of the protease. While the remaining AutoDock Vina v1.2.2 settings were left at their default values, the number of solutions was fixed at 10. An internal Python script was used to carry out the virtual screening simulation (Hakmi et al. 2020).

The method was followed for the remaining receptors, with the exception that the centre and size were different. Beta M^{Pro} receptor center = (-11.252, 0.617, 10.563), size = 98×98×116 Angstroms. Lambda M^{Pro} receptor center = (-2.018, 0.295, 11.516), size = 94×78×126 Angstroms. Omicron M^{Pro} receptor center = (1.167, -4.000, 27.611), size = 82×78×124 Angstroms.

PADLE, THE PERL IDE FOR VIRTUAL DOCKING

Padle, the Perl IDE (https://padre.perlide.org), is a run command that supports AutoDock Vina v1.2.2 to executing mass docking of 100 ligands against a single receptor. There were four simulations carried out individually for wild, beta, lambda, and omicron M^{Pro} with the 100 ligands. After checking that the correct file was in use, the **perl – v** command was being typed in Command Prompt to install Perl for programming. The Perl script file was saved as "Vina_windows.pl" in the same folder called "docking-wild" that contains "vina", "vina_license", "vina_split", "receptor.pdbqt", and all the 100 "ligand.pdbqt", "conf_vs" files. A new empty text document file was created as "Ligand.txt" to accommodate the docking outcome. A series of command was initialised in a new Command Prompt window to initiate the mass docking. Depending on the size of the input files and the computer response, the mass docking was run automatically for approximately two to three hours. It is important to note that the command is case-sensitive, a typo will prevent the action from progressing to the next step. Upon completion, the output log files were found in "Ligand.txt" folder.

OUTPUT ANALYSIS

PyMOL was utilised to generate receptor-ligand complex by loading the receptor (6Y2E) and the selected ligand from the saved files. From the docked ligand output, mode 1, the best-docked model, was chosen. The pre-treated complex was carried forward to the next step of interaction analysis. Similarly, the method was carried out for 7U29, 7U28, and 7TLL. PyMOL 2.5.2 was obtained under the terms of an educational use registration licence (https://pymol.org/edu/).

BIOVIA discovery studio visualizer by Dassault Systemes is a free modelling application used for protein and small molecule analysis (https://discover.3ds.com/

discovery-studio-visualizer-download). The receptor-ligand complex was opened in the discovery studio visualizer to study the ligand interaction. The software feature allows intensive residue labelling. The interaction show type was selected as "conventional = hydrogen bonding". The hydrogen bonding was depicted on the receptor surface. The interaction was also set to be displayed as a 2D graphic.

RESULTS

The docking results were prompted in the form of a binding affinity (kcal/mol) scoring system. Among the 10 binding modes generated by AutoDock Vina v1.2.2, the strongest binding affinity of the ligand-receptor was chosen. The ligands with the highest docking scores, in the top 20%, were tabulated and compared among the M^{Pro} of the four SARS-CoV-2 variants, wild, beta, lambda, and omicron. Only the highlighted ligands that fall into this range were narrowed down for further interaction study. The binding affinity of the ligands and various M^{Pro} ranges from -8.1 kcal/mol to -9.2 kcal/mol as listed in Table 1. The most consistent score was seen in ligand 3, 10, and 89, across all variant M^{Pro}.

Interaction analysis was performed on the 10 ligands with the highest binding affinity to study. Ligands 3 and 10 show consistent interactions with all four M^{Pro} variants. Each wild and mutant type of SARS-CoV-2 main protease (M^{Pro}) receptor-ligand interaction was displayed in 3D and 2D planes. The types of interactions, attractive charge, salt bridge, conventional hydrogen bonding, carbon hydrogen bonding, alkyl, π-interaction, and π-π stacking were listed in Table 2, along with the residues involved in all four studied variants.

The interaction analysis of ligand 3 against SARS-CoV-2 M^{Pro} variants is illustrated in Figure 4. There were six types of bindings shown in wild-type M^{Pro} with ligand 3. They were unfavourable bump, unfavourable positive-positive, unfavourable donor-donor, attractive charge, conventional hydrogen bond, and π-alkyl. Residues LYS 137 and ASN 133 were involved in unfavourable bump formation, LYS 137 in unfavourable positive-positive, ASN 133 in unfavourable donor-donor, ASP 197 and LYS 5 in attractive charge, ASP 197, THR 135, ARG 131, THR 199 and ASP 289 in conventional hydrogen bonding, and LEU 287 in π-alkyl interaction. Whilst in the interaction with beta M^{Pro}, five types of bindings were formed. They were attractive charge, conventional hydrogen bond, carbon hydrogen bond, unfavourable donor-donor, and π-alkyl. Residue LYS 137 was involved in attractive charge, THR 199, GLY 195, ASP 289, ASN 238 and ASP 197 in conventional hydrogen bonding, ASN 133 in unfavourable donor-donor, and LEU 286 and LEU 287 in π-alkyl interaction. Binding with lambda M^{Pro} formed six types of bindings. They were unfavourable bump, salt bridge and attractive charge, conventional hydrogen bond, carbon hydrogen bond, π-donor hydrogen bond, and π-sigma. Residue TYR 239 was involved in unfavourable bump, ASP 197, LYS 137 and ARG 131 in salt bridge and attractive charge, THR 199, ASP 289 and GLY 195 in conventional hydrogen bond, ASP 197 in carbon hydrogen bonding, and LEU 287 π-donor hydrogen bond. Residue interacted with π-sigma was unknown. The binding of omicron M^{Pro} formed four types of bindings. They were unfavourable bump, attractive charge, conventional hydrogen bond, and π-alkyl. Residue ASN 133 was involved in unfavourable bump formation, ASP 197 in attractive charge, THR 135, ASP 197, ASN 238 and ASP 289 in conventional hydrogen bond, and LEU 287 in π-alkyl interaction.

The interaction analysis of ligand 10 against SARS-CoV-2 M^{Pro} variants is illustrated in Figure 5. There were three types of bindings shown in wild-type and beta M^{Pro} with ligand 10. They were conventional hydrogen bond, π-π stacked, and π-alkyl. Residues ILE 152 and PHE 294 were involved in conventional hydrogen bonding, PHE 294 in π-π stacked, and VAL 202, ILE 249 and PRO 294 in π-alkyl interaction. Interaction with lambda M^{Pro} formed five types of bindings. They were attractive charge, conventional hydrogen bond, carbon hydrogen bond, π-π stacked, and π-alkyl. Residue ASP 295 was involved in attractive charge formation, HIS 246 and GLU 240 in conventional hydrogen bonding, PRO 293 in carbon hydrogen bonding, HIS 246 in π-π stacked, and ILE 249 and VAL 202 in π-alkyl interaction. Whilst the binding with omicron M^{Pro} developed two types of bindings. They were π-sigma and π-alkyl. Residue PHE 294 was involved in π-sigma, and ILE 249, VAL 202, PRO 293, VAL 297 and PRO 252 in π-alkyl interaction.

DISCUSSION

The prediction of small molecular inhibitors for different SARS-CoV-2 variants varied upon the target site receptor's 3D conformation and the interaction with the tested drugs. This study aims to investigate small molecular inhibitors that have the potential to inhibit the enzymatic activity of SARS-CoV-2 main protease (M^{Pro}) in different variants; wild, beta, lambda, and omicron. All of the 10 ligands are the best-scored candidates targeting the variant M^{Pro}. Besides the two propound inhibitors, ergotamine, benzamidine, argifin, irinotecan, dihydroergotamine, telmisartan, bromocriptine, and cilengitide have also shown significant scores ranging from -8.1 kcal/mol to -9.2 kcal/mol, while some studies considered the docking score with a higher cutoff, for instance -6.5 kcal/mol (Hosseini et al. 2021; Shah, Modi & Sagar 2020).

TABLE 1. Ten best small molecule inhibitors with strongest binding affinities for SARS-CoV-2 main protease (M^{Pro}), wild, beta, lambda and, omicron

Ligand number	Small molecule inhibitors	SARS-CoV-2 variant M^{Pro} binding affinity (kcal/mol)			
		Wild	Beta	Lambda	Omicron
2	Ergotamine	-8.6	-9.2	-9	-8.5
3	2,5-Dibenzyloxy-3-hydroxyligand-hexanedioic acid bis-[(2-hydroxy-indan-1-YL)-amide]	-8.7	-8.3	-8.5	-8.2
10	Remetinostat	-8.3	-8.6	-8.4	-8.1
11	Benzamidine	-8.2	-9	-8.8	-8.5
15	Argifin	-8.2	-8.8	-9	-7.9
29	Irinotecan	-8.1	-8.8	-9	-8.1
31	Dihydroergotamine	-9.2	-9.1	-8.9	-8.6
35	Telmisartan	-8.7	-8.5	-8.6	-8.1
82	Bromocriptine	-8.7	-8.5	-8.8	-8
89	Cilengitide	-8.7	-8.4	-8.5	-8.2

TABLE 2. Types of interactions and residues involved in binding of ligands 3 and 10 with M^{Pro} variants. Through the common interactions and residues involved, these two ligands interacted consistently with all four M^{Pro} variants

Common interacted residues	Binding type of SARS-CoV-2 variant M^{Pro}			
	Wild	Beta	Lambda	Omicron
LIGAND 3				
ASP 289	Conventional hydrogen bonding			
ASP 197	Attractive charge	-	Attractive charge	Attractive charge
	Conventional hydrogen bond	Carbon hydrogen bond	Carbon hydrogen bond	Conventional hydrogen bond
LEU 287	π-alkyl	π-alkyl	-	π-alkyl
	-	-	π-donor hydrogen bond	-
LIGAND 10				
PRO 293	π-alkyl	π-alkyl	-	π-alkyl
	-	-	Carbon hydrogen bond	-
VAL 202	π-alkyl			
ILE 249	π-alkyl			

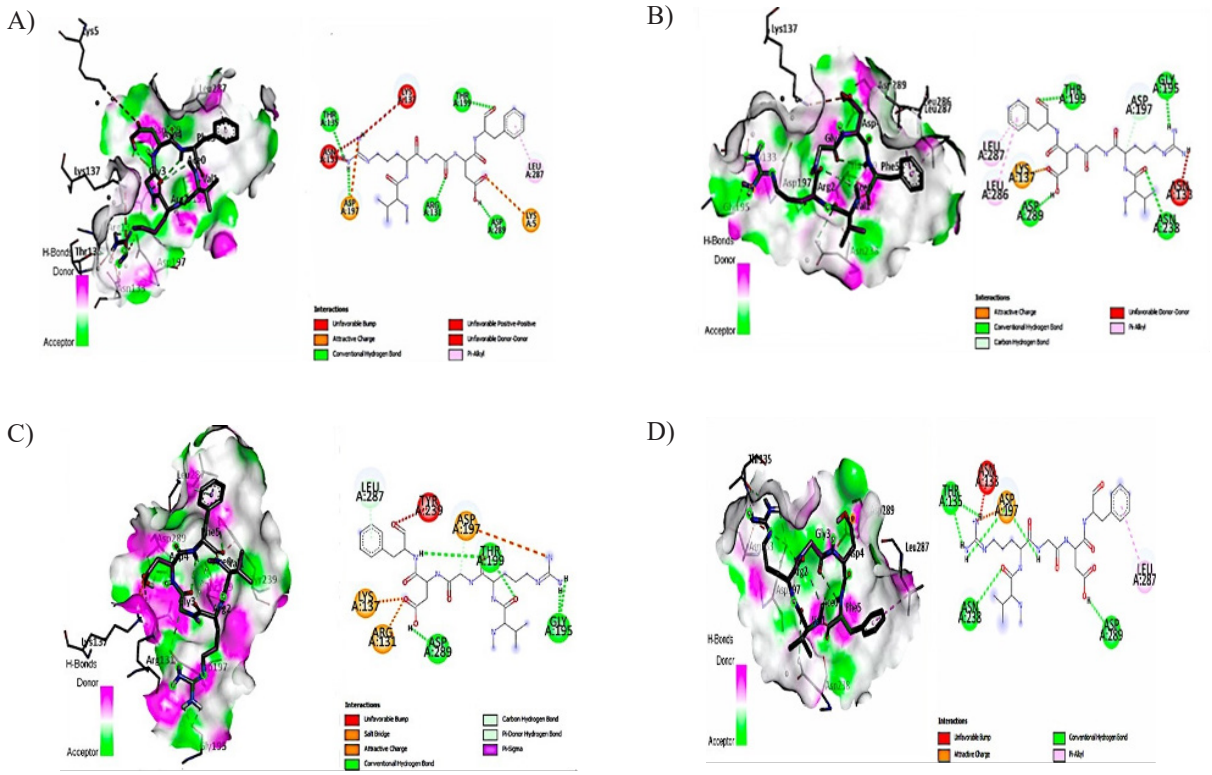

FIGURE 4. The interactions of ligand 3 against SARS-CoV-2 M^{Pro} of wild (A), beta (B), lambda (C) and, omicron (D) shown in the 3D catalytic pocket and 2D plane

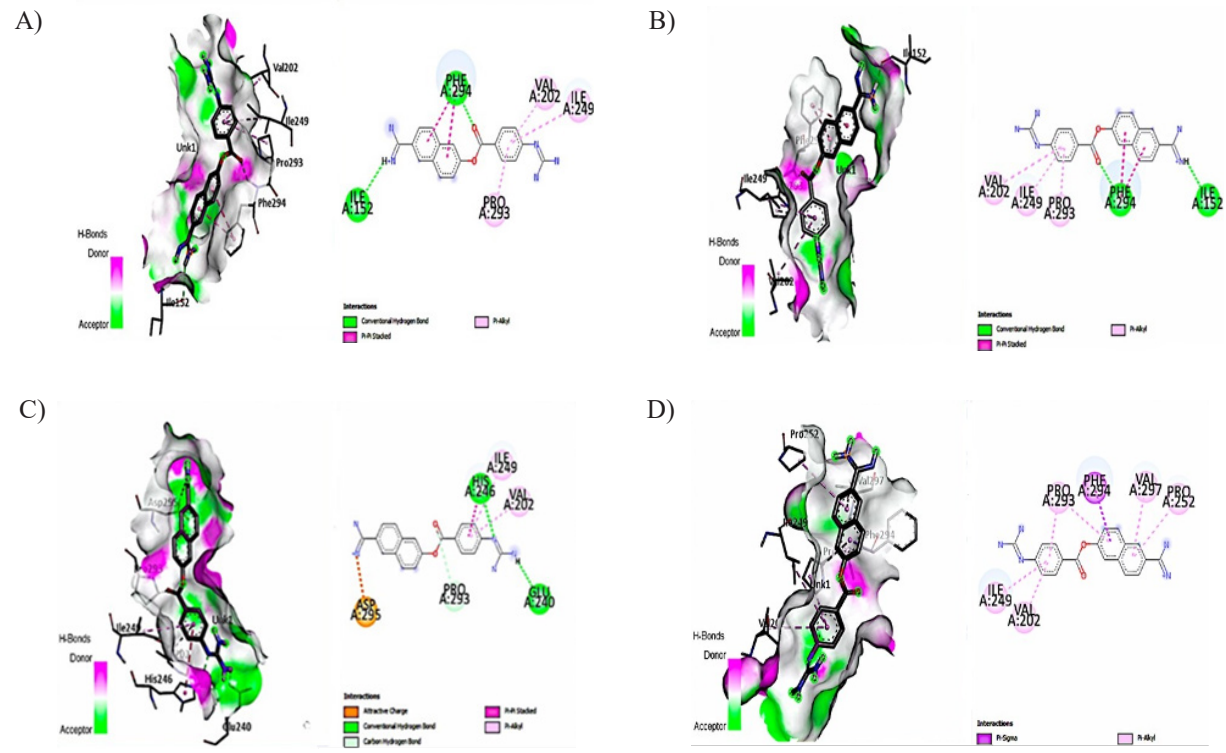

FIGURE 5. The interactions of ligand 10 against SARS-CoV-2 MPro of wild (A), beta (B), lambda (C) and, omicron (D) shown in the 3D catalytic pocket and 2D plane

Ergotamine (ligand 2) and its derivative dihydroergotamine (ligand 31), both FDA-approved for managing headaches and migraines, have garnered attention for their potential in treating MERS and SARS-CoV-2. They target the main protease (M^{Pro}) of the coronavirus, directly interacting with critical residues like CYS 145 and HIS 41 (Gul et al. 2021; Gurung et al. 2020). This interaction is crucial for inhibiting the enzyme's monomeric form and potentially disrupting the virus's replication cycle.

Benzamidine, typically used to treat mouth infections and gingivitis, has also shown promise as an inhibitor of SARS-CoV-2 M^{Pro} (Santos-Filho et al. 2020). It interacts with the enzyme through alkyl interactions, though some interactions may be unfavorable. Cilengitide (ligand 89), an investigational medicine primarily studied for its potential in treating lung cancer, has demonstrated antagonistic effects on blood vessels, reducing the risk of SARS-CoV-2 infection (Nader et al. 2021; Zheng et al. 2022). Both agrifin (ligand 15) and cilengitide engage in conventional hydrogen bonding and π-alkyl interactions with M^{Pro} variants, with cilengitide also forming attractive charges and salt bridges.

Irinotecan, a topoisomerase 1 inhibitor primarily used to treat colorectal cancer, has shown efficacy in treating critical COVID-19 patients (Gurung et al. 2020; Lovetrue 2020). *In-silico* studies suggest that irinotecan's interaction with M^{Pro} involves conventional hydrogen bonding and carbon hydrogen bonding interactions. Telmisartan (ligand 35), an angiotensin receptor blocker prescribed for heart conditions, has shown promise as a COVID-19 therapeutic (Duarte et al. 2021; Rothlin et al. 2021). It primarily engages in conventional hydrogen bonding interactions when docked against M^{Pro} variants. Bromocriptine (ligand 82), an FDA-approved dopamine D2 receptor agonist for early Parkinson's syndrome, may also allosterically inhibit SARS-CoV-2 M^{Pro}, with interactions involving conventional hydrogen bonding and alkyl interactions. The drug unravelled the possible allosteric inhibition of SARS-CoV-2 main protease on E290, F291, E288, D289 beside the active site (Yuce et al. 2021).

Out of 10 potential inhibitors of M^{Pro} predicted in this study, ligand 3 (2,5-Dibenzyloxy-3-hydroxyligand-hexanedioic acid bis-[(2-hydroxy-indan-1-YL)-amide]) and remetinostat shared the highest similarities in the interaction with M^{Pro} receptors and the types of binding for all variants. The key residues that participate in the ligand-receptor interaction of ligand 3 are ASP 289, ASP 197, and LEU 287. Residue ASP 289 of all four variants displayed conventional hydrogen bonding. Residue ASP 197 forms electrostatic forces in wild, lambda, and omicron, conventional hydrogen bonding in wild and omicron M^{Pro}, and carbon-hydrogen bonding in beta and lambda. Residue LEU 287 demonstrated π-alkyl interaction with wild, beta and omicron M^{Pro}, and π-donor hydrogen bonding in lambda M^{Pro}. This potential ligand is a Gag polyprotein inhibitor targeting HIV-1 viral maturation. By inhibiting Gag-pol, the subsequent virion assembly including envelop protein recruitment and viral RNA packaging will be altered, causing immature or loss-of-function virion production.

As for remetinostat, the key residues that participate in the ligand-receptor interaction are PRO 293, VAL 202, and ILE 249. VAL 202 and ILE 249 in all variants displayed π-alkyl interaction with the respective ligand. With residue PRO 293, π-alkyl interaction was shown in wild, beta, and omicron M^{Pro}, while carbon-hydrogen bonding in lambda M^{Pro}. Remetinostat is a cancer suppressor medication being tested in humans in phases I and/or II for the treatment of skin cancer. Even though remetinostat is prescribed for external use, it is highly effective towards SARS-CoV-2 M^{Pro} and the variants via molecular docking and hence, worth the attention as toxicity factor influences oral medication. No study has been reported on the use of remetinostat in SARS-CoV-2 treatment. The drug is labelled as a novel adjuvant treatment and paired with chemotherapy to treat cancer patients.

The main types of interactions formed are attractive charges, salt bridges, conventional hydrogen bonds, carbon hydrogen bonds, and various π-interactions. Attractive charges and salt bridges were observed by residues LSY 5, ASP 197, LYS 137, and ARG 131 with cilengitide and 2,5-Dibenzyloxy-3-hydroxyligand-hexanedioic acid bis-[(2-hydroxy-indan-1-YL)-amide]. The electrostatic attractions are formed by two oppositely charged residues, N (positive) and O (negative) (Bosshard, Marti & Jelesarov 2004), though salt bridges and attractive charges are occasionally linked. In comparison to other molecular interactions, salt-bridge, π-cation, and amide bridge interactions are considerably stronger due to their extremely high interaction energies (Xie et al. 2015). Strong bonds, however, do not always equate to effective interactions in drug design; instead, elements including the pH of the solvent, ionic interactions, and the mode of mechanism of drug determine effectiveness. In order to stabilise a drug at the interface of a receptor site, weak intermolecular interactions have a significant impact on the binding affinity between ligand-receptor complexes (Yunta 2017).

Common residues that display hydrogen bonding are THR 26, THR 135, THR 199, HIS 246, HIS 41, HIS 163, THR 190, GLU 166, GLY 195, GLY 143, GLN 110, GLU 166, ARG 131, ASP 289, ASN 238, ALA 194, CYS 145, ASN 142, PHE 294, and LEU 141. In most cases, the residues are found to recur in other M^{Pro} variants hydrogen bonding with ligands. This is because the specificity of

ligand binding is greatly influenced by conventional hydrogen bond (NH-O, OH-O, OH-N, and NH-N) (Horowitz & Trievel 2012; Wade & Goodford 1989). The formation of hydrogen bonds between two distinct molecules promotes drug precipitation and crystal packing (Saluja et al. 2016). Hydrogen bonding which is a type of dipole-dipole interaction is weaker than electrostatic forces but stronger than van der Waals interaction. In comparison to the lower electronegativity of oxygen and nitrogen, carbon has not generally been recognised as a standard hydrogen bond donor. Nevertheless, numerous investigations have shown that even aliphatic carbon atoms can form weak hydrogen bonds, which are referred to as CH-O hydrogen bonds (Steiner 2002; Steiner & Desiraju 1998).

The low molecular weight ligands, both natural and synthetic, attach to receptors in a variety of non-covalent interactions, primarily with the side chains of residues in the enzymes' binding pockets (Brylinski 2018). In this study, most π-interactions express as hydrophobic interactions and are a type of London dispersion forces. These interactions, including those that contribute to aromatic stacking, significantly influence the stability, efficacy, and functionality of a drug (Hwang et al. 2015). In addition, alkyl and π-alkyl interactions are formed in omicron M^{Pro} via the free electron cloud surrounding the unsaturated carbon atom of the molecule, attracting to the opposite partial positively charged residues.

CONCLUSION

In light of the COVID-19 pandemic, molecular docking facilitates the development of lead compounds through virtual screening. Ten potential small molecule inhibitors, ergotamine, 2,5-Dibenzyloxy-3-hydroxyligand-hexanedioic acid bis-[(2-hydroxy-indan-1-YL)-amide], remetinostat, benzamidine, argifin, irinotecan, dihydroergotamine, telmisartan, bromocriptine, and cilengitide, were predicted in this study. Two of the potential inhibitors, 2,5-Dibenzyloxy-3-hydroxyligand-hexanedioic acid bis-[(2-hydroxy-indan-1-YL)-amide] and remetinostat, interacted with SARS-CoV-2 main protease of all four variants consistently.

ACKNOWLEDGEMENTS

The work has been funded by the Universiti Sains Malaysia (Short-term Research Grant) No. 304/PBIOLOGI/6315612 granted to NII.

REFERENCES

Adedeji, A.O. & Sarafianos, S.G. 2014. Antiviral drugs specific for coronaviruses in preclinical development. *Current Opinion in Virology* 8: 45-53.

Anand, K., Ziebuhr, J., Wadhwani, P., Mesters, J.R. & Hilgenfeld, R. 2003. Coronavirus main proteinase (3CLpro) structure: Basis for design of anti-SARS drugs. *Science* 300(5626): 1763-1767.

Bosshard, H.R., Marti, D.N. & Jelesarov, I. 2004. Protein stabilization by salt bridges: Concepts, experimental approaches and clarification of some misunderstandings. *Journal of Molecular Recognition* 17(1): 1-16.

Brylinski, M. 2018. Aromatic interactions at the ligand–protein interface: Implications for the development of docking scoring functions. *Chemical Biology & Drug Design* 91(2): 380-390.

Bzówka, M., Mitusińska, K., Raczyńska, A., Samol, A., Tuszyński, J.A. & Góra, A. 2020. Structural and evolutionary analysis indicate that the SARS-CoV-2 Mpro is a challenging target for small-molecule inhibitor design. *International Journal of Molecular Sciences* 21(9): 3099.

Chia, C.B., Xu, W. & Shuyi Ng, P. 2022. A patent review on SARS coronavirus main protease (3CLpro) inhibitors. *ChemMedChem* 17(1): e202100576.

Duarte, M., Pelorosso, F., Nicolosi, L.N., Salgado, M.V., Vetulli, H., Aquieri, A., Azzato, F., Castro, M., Coyle, J., Davolos, I., Fernandez Criado, I., Gregori, R., Mastrodonato, P., Rubio, M.C., Sarquis, S., Wahlmann, F. & Rothlin, R.P. 2021. Telmisartan for treatment of COVID-19 patients: An open multicenter randomized clinical trial. *EClinicalMedicine* 37: 100962.

Flynn, J.M., Zvornicanin, S.N., Tsepal, T., Shaqra, A.M., Kurt Yilmaz, N., Jia, W., Moquin, S., Dovala, D., Schiffer, C.A. & Bolon, D.N.A. 2023. Contributions of hyperactive mutations in Mpro from SARS-CoV-2 to drug resistance. *ACS Infectious Diseases* 10(4): 1174-1184.

Gentile, F., Yaacoub, J.C., Gleave, J., Fernandez, M., Ton, A.T., Ban, F., Stern, A. & Cherkasov, A. 2022. Artificial intelligence–enabled virtual screening of ultra-large chemical libraries with deep docking. *Nature Protocols* 17(3): 672-697.

Govardhanagiri, S., Bethi, S. & Nagaraju, G.P. 2019. Small molecules and pancreatic cancer trials and troubles. In *Breaking Tolerance to Pancreatic Cancer Unresponsiveness to Chemotherapy*, edited by Nagaraju, G.P. London: Academic Press. pp. 117-131.

Goyal, B. & Goyal, D. 2020. Targeting the dimerization of the main protease of coronaviruses: A potential broad-spectrum therapeutic strategy. *ACS Combinatorial Science* 22(6): 297-305.

Greasley, S.E., Noell, S., Plotnikova, O., Ferre, R., Liu, W., Bolanos, B., Fennell, K., Nicki, J., Craig, T., Zhu, Y., Stewart, A.E. & Steppan, C.M. 2022. Structural basis for the *in vitro* efficacy of nirmatrelvir against SARS-CoV-2 variants. *Journal of Biological Chemistry* 298(6): 101972.

Gul, S., Ozcan, O., Asar, S., Okyar, A., Barıs, I. & Kavakli, I.H. 2021. *In silico* identification of widely used and well-tolerated drugs as potential SARS-CoV-2 3C-like protease and viral RNA-dependent RNA polymerase inhibitors for direct use in clinical trials. *Journal of Biomolecular Structure and Dynamics* 39(17): 6772-6791.

Gurung, A.B., Ali, M.A., Lee, J., Farah, M.A. & Al-Anazi, K.M. 2020. *In silico* screening of FDA approved drugs reveals ergotamine and dihydroergotamine as potential coronavirus main protease enzyme inhibitors. *Saudi Journal of Biological Sciences* 27(10): 2674-2682.

Hakmi, M., Bouricha, E.M., Kandoussi, I., El Harti, J. & Ibrahimi, A. 2020. Repurposing of known anti-virals as potential inhibitors for SARS-CoV-2 main protease using molecular docking analysis. *Bioinformation* 16(4): 301-306.

Higueruelo, A.P., Schreyer, A., Bickerton, G.R.J., Pitt, W.R., Groom, C.R. & Blundell, T.L. 2009. Atomic interactions and profile of small molecules disrupting protein–protein interfaces: The TIMBAL database. *Chemical Biology & Drug Design* 74(5): 457-467.

Horowitz, S. & Trievel, R.C. 2012. Carbon-oxygen hydrogen bonding in biological structure and function. *Journal of Biological Chemistry* 287(50): 41576-41582.

Hosseini, M., Chen, W., Xiao, D. & Wang, C. 2021. Computational molecular docking and virtual screening revealed promising SARS-CoV-2 drugs. *Precision Clinical Medicine* 4(1): 1-16.

Huang, H., Zhang, G., Zhou, Y., Lin, C., Chen, S., Lin, Y., Mai, S. & Huang, Z. 2018. Reverse screening methods to search for the protein targets of chemopreventive compounds. *Frontiers in Chemistry* 6: 138.

Hung, Y.P., Lee, J.C., Chiu, C.W., Lee, C.C., Tsai, P.J., Hsu, I.L. & Ko, W.C. 2022. Oral Nirmatrelvir/ Ritonavir therapy for COVID-19: The dawn in the dark? *Antibiotics* 11(2): 220.

Hwang, J., Dial, B. E., Li, P., Kozik, M. E., Smith, M. D., & Shimizu, K. D. (2015). How important are dispersion interactions to the strength of aromatic stacking interactions in solution? *Chemical Science*, *6*(7), 4358-4364.

Khalifa, H.O. & Al Ramahi, Y.M. 2024. After the hurricane: Anti-COVID-19 drugs development, molecular mechanisms of action and future perspectives. *International Journal of Molecular Sciences* 25(2): 739.

Khan, S.L., Siddiqui, F.A., Jain, S.P. & Sonwane, G.M. 2021. Discovery of potential inhibitors of SARS-CoV-2 (COVID-19) main protease (Mpro) from *Nigella sativa* (black seed) by molecular docking study. *Coronaviruses* 2(3): 384-402.

Kneller, D.W., Phillips, G., O'Neill, H.M., Jedrzejczak, R., Stols, L., Langan, P., Joachimiak, A., Coates, L. & Kovalevsky, A. 2020. Structural plasticity of SARS-CoV-2 3CL Mpro active site cavity revealed by room temperature X-ray crystallography. *Nature Communications* 11(1): 3202.

Lam, C. & Patel, P. 2023. *Nirmatrelvir-Ritonavir.* In StatPearls [Internet]. StatPearls Publishing.

Lee, J., Worrall, L.J., Vuckovic, M., Rosell, F.I., Gentile, F., Ton, A.T., Cavaney, N.A., Ban, F., Cherkasov, A., Paetzel, M. & Strynadka, N.C.J. 2020. Crystallographic structure of wild-type SARS-CoV-2 main protease acyl-enzyme intermediate with physiological C-terminal autoprocessing site. *Nature Communications* 11: 5877.

Li, Z., Li, X., Huang, Y.Y., Wu, Y., Liu, R., Zhou, L., Lin, Y., Wu, D., Zhang, L., Liu, H., Xu, X., Yu, K., Zhang, Y., Cui, J., Zhan, C.G., Wang, X. & Luo, H.B. 2020. Identify potent SARS-CoV-2 main protease inhibitors via accelerated free energy perturbation-based virtual screening of existing drugs. *Proceedings of the National Academy of Sciences* 117(44): 27381-27387.

Lovetrue, B. 2020. The AI-discovered aetiology of COVID-19 and rationale of the irinotecan+ etoposide combination therapy for critically ill COVID-19 patients. *Medical Hypotheses* 144: 110180.

Morse, J.S., Lalonde, T., Xu, S. & Liu, W.R. 2020. Learning from the past: possible urgent prevention and treatment options for severe acute respiratory infections caused by 2019-nCoV. *Chembiochem*. 21(5): 730-738.

Muppalaneni, N.B. & Rao, A.A. 2011. PDBToSDF: Create ligand structure files from PDB file. *Bioinformation* 6(10): 383.

Nader, D., Fletcher, N., Curley, G.F. & Kerrigan, S.W. 2021. SARS-CoV-2 uses major endothelial integrin αvβ3 to cause vascular dysregulation *in-vitro* during COVID-19. *PLoS ONE* 16(6): e0253347.

Nutho, B., Mahalapbutr, P., Hengphasatporn, K., Pattaranggoon, N.C., Simanon, N., Shigeta, Y., Hannongbua, S. & Rungrotmongkol, T. 2020. Why are lopinavir and ritonavir effective against the newly emerged coronavirus 2019? Atomistic insights into the inhibitory mechanisms. *Biochemistry* 59(18): 1769-1779.

Odhar, H.A., Ahjel, S.W., Albeer, A.A.M.A., Hashim, A.F., Rayshan, A.M. & Humadi, S.S. 2020. Molecular docking and dynamics simulation of FDA approved drugs with the main protease from 2019 novel coronavirus. *Bioinformation* 16(3): 236-244.

Ordog, R., Szabadka, Z. & Grolmusz, V. 2009. DECOMP: A PDB decomposition tool on the web. *Bioinformation* 3(10): 413-414.

Pang, X., Xu, W., Liu, Y., Li, H. & Chen, L. 2023. The research progress of SARS-CoV-2 main protease inhibitors from 2020 to 2022. *European Journal of Medicinal Chemistry* 257: 115491.

Rothlin, R.P., Duarte, M., Pelorosso, F.G., Nicolosi, L., Salgado, M.V., Vetulli, H.M. & Spitzer, E. 2021. Angiotensin receptor blockers for COVID-19: Pathophysiological and pharmacological considerations about ongoing and future prospective clinical trials. *Frontiers in Pharmacology* 12: 603736.

Saluja, H., Mehanna, A., Panicucci, R. & Atef, E. 2016. Hydrogen bonding: Between strengthening the crystal packing and improving solubility of three haloperidol derivatives. *Molecules* 21(6): 719.

Santos-Filho, O.A., Eynde, J.J.V., Mayence, A. & Huang, T.L. 2020. Evaluation of aryl amidines/benzimidazoles as potential anti-COVID-19 agents: A computational study. https://doi.org/10.3390/ECMC2020-07288

Shah, B., Modi, P. & Sagar, S.R. 2020. *In silico* studies on therapeutic agents for COVID-19: Drug repurposing approach. *Life Sciences* 252: 117652.

Steiner, T. 2002. The hydrogen bond in the solid state. *Angewandte Chemie International Edition* 41(1): 48-76.

Steiner, T. & Desiraju, G.R. 1998. Distinction between the weak hydrogen bond and the van der Waals interaction. *Chemical Communications* 8: 891-892.

ul Qamar, M.T., Alqahtani, S.M., Alamri, M.A. & Chen, L.L. 2020. Structural basis of SARS-CoV-2 3CLpro and anti-COVID-19 drug discovery from medicinal plants. *Journal of Pharmaceutical Analysis* 10(4): 313-319.

Vatansever, E.C., Yang, K.S., Drelich, A.K., Kratch, K.C., Cho, C.C., Kempaiah, K.R., Hsu, J.C., Mellott, D.M., Xu, S., Tseng, C-T.K. & Liu, W.R. 2021. Bepridil is potent against SARS-CoV-2 *in vitro*. *Proceedings of the National Academy of Sciences* 118(10): e2012201118.

Wade, R.C. & Goodford, P.J. 1989. The role of hydrogen-bonds in drug binding. *Progress in Clinical and Biological Research* 289: 433-444.

Xiang, R., Yu, Z., Wang, Y., Wang, L., Huo, S., Li, Y., Liang, R., Hao, Q., Ying, T., Gao, Y., Yu, F. & Jiang, S. 2022. Recent advances in developing small-molecule inhibitors against SARS-CoV-2. *Acta Pharmaceutica Sinica B* 12(4): 1591-1623.

Xie, N.Z., Du, Q.S., Li, J.X. & Huang, R.B. 2015. Exploring strong interactions in proteins with quantum chemistry and examples of their applications in drug design. *PLoS ONE* 10(9): e0137113.

Xiong, R., Zhang, L., Li, S., Sun, Y., Ding, M., Wang, Y., Zhao, Y., Wu, Y., Shang, W., Jiang, X., Shan, J., Shen, Z., Tong, Y., Xu, L., Chen, Y., Liu, Y., Zou, G., Lavillete, D., Zhao, Z., Wang, R., Zhu, L., Xiao, G., Lan, K., Li, H. & Xu, K. 2020. Novel and potent inhibitors targeting DHODH are broad-spectrum antivirals against RNA viruses including newly-emerged coronavirus SARS-CoV-2. *Protein & Cell* 11(10): 723-739.

Yuce, M., Cicek, E., Inan, T., Dag, A.B., Kurkcuoglu, O. & Sungur, F.A. 2021. Repurposing of FDA-approved drugs against active site and potential allosteric drug-binding sites of COVID-19 main protease. *Proteins: Structure, Function, and Bioinformatics* 89(11): 1425-1441.

Yunta, M.J. 2017. It is important to compute intramolecular hydrogen bonding in drug design. *Am. J. Model. Optim*. 5(1): 24-57.

Zhang, L., Lin, D., Sun, X., Curth, U., Drosten, C., Sauerhering, L., Becker, S., Rox, K. & Hilgenfeld, R. 2020. Crystal structure of SARS-CoV-2 main protease provides a basis for design of improved α-ketoamide inhibitors. *Science* 368(6489): 409-412.

Zheng, J., Zhang, Y., Zhao, H., Liu, Y., Baird, D., Karim, M.A., Ghoussaini, M., Schwartzentruber, J., Dunham, I., Elsworth, B., Roberts, K., Compton, H., Miller-Molloy, F., Liu, X., Wang, L., Zhang, H., Smith, G.D. & Gaunt, T.R. 2020. Multi-ancestry Mendelian randomization of omics traits revealing drug targets of COVID-19 severity. *eBioMedicine* 81: 104112. https://doi.org/10.1016/j.ebiom.2022.104112

*Corresponding author; email: nurul.ismail@usm.my